Planetary Boundary Layer Parameterization

Reference Materials

The following lecture material draws extensively from Chapter 5 of *Parameterization Schemes* by David Stensrud. The course text provides a reasonably robust summary of this information. *An Introduction to Boundary Layer Meteorology* by Roland Stull is a recommended resource for more information regarding boundary layer processes and is often cited by the Stensrud text.

Overview of the Planetary Boundary Layer

The *planetary boundary layer*, or PBL, is the layer over which the influence of the Earth's surface is directly transmitted to the free atmosphere. The vertical extent of turbulent mixing defines the top of the PBL; it can extend upward of several kilometers above the surface during the local daytime hours but be confined to within 100 m or less of the surface at night. An *inversion* often separates the PBL from the free atmosphere. The PBL is a turbulent, mixed layer characterized by sub-grid-scale turbulent eddies that transport heat, moisture, and momentum vertically. Turbulent eddies may result from either *buoyancy* or *vertical wind shear*.

Buoyancy refers to the local instability generated by sensible and latent heat fluxes directed from the underlying surface to the atmosphere. The magnitude of these heat fluxes is strongly dependent upon underlying surface characteristics. The release of the local instability results in the generation of *thermals*, or vertical plumes of buoyant air, extending over the depth of the PBL. The upward momentum possessed by thermals enables them to overshoot their level of neutral buoyancy, typically found at the top of the PBL where potential temperature rapidly increases with height. It is across this inversion layer that the PBL entrains environmental air from the free atmosphere as thermals sink back into the PBL. Turbulence within the PBL itself ensures that air from the free atmosphere is quickly mixed with the air that comprises the PBL.

During the local daytime hours, buoyancy is the primary contributor to PBL turbulence. At night, however, vertical wind shear is the primary contributor to PBL turbulence. Although vertical wind shear may contribute to turbulence during local daytime, buoyancy does not contribute to PBL turbulence during local nighttime when radiative cooling dominates the surface radiation budget. Turbulence driven by vertical wind shear is known as *mechanical* turbulence and is intermittent relative to the more continuous turbulence in the buoyancy-driven daytime PBL.

The evolution of the PBL over a series of several diurnal cycles is illustrated in Figure 1. Idealized schematics of the daytime and nocturnal PBLs are provided in Figures 2 and 3, respectively. A boundary layer parameterization must be able to accurately reproduce both daytime and nocturnal PBLs under a wide range of atmospheric conditions.

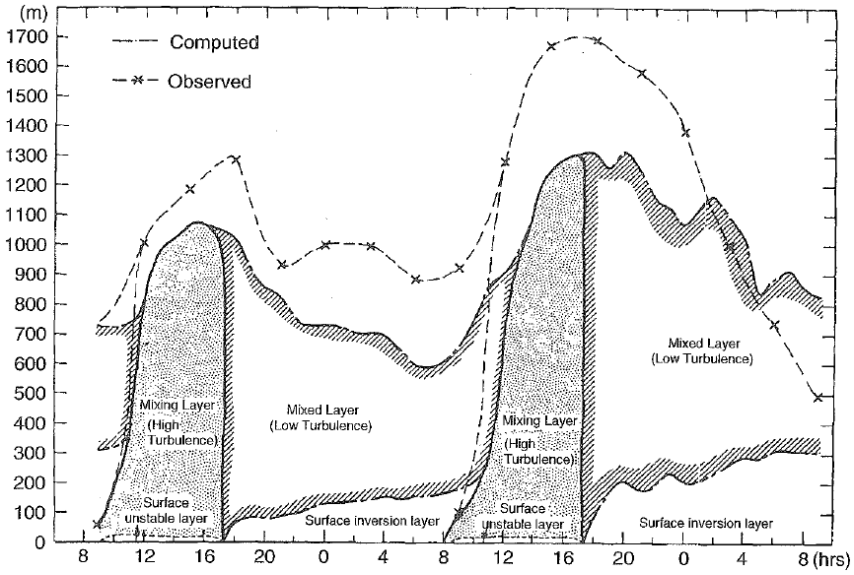

Figure 1. Schematic of PBL evolution over the course of two full diurnal cycles. During the local daytime hours, the turbulent mixed layer grows to in excess of 1 km in depth. As day turns to night, PBL turbulence weakens, leaving behind a residual mixed layer atop a near-surface inversion layer that forms in response to radiative cooling. The near-surface inversion layer deepens slowly at night as the effects of radiative cooling are episodically interrupted by mechanical turbulence. At the same time, the residual mixed layer shrinks in vertical extent due to internal friction as the evening progresses. Figure reproduced from Stensrud (2007), their Figure 5.1.

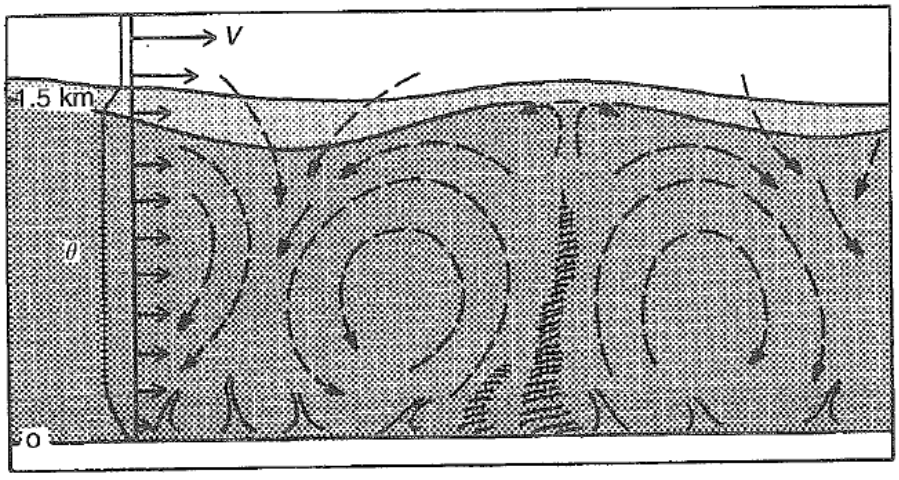

Figure 2. Artistic rendering of an idealized daytime PBL. Here, organized thermals act in concert with turbulent eddies to homogenize potential temperature, momentum, and moisture within the PBL. Entrainment occurs at the top of the PBL as thermals overshoot their level of neutral buoyancy and subsequently sink back into the PBL. Subtle horizontal variations in PBL height are also depicted. Figure reproduced from Stensrud (2007), their Figure 5.5.

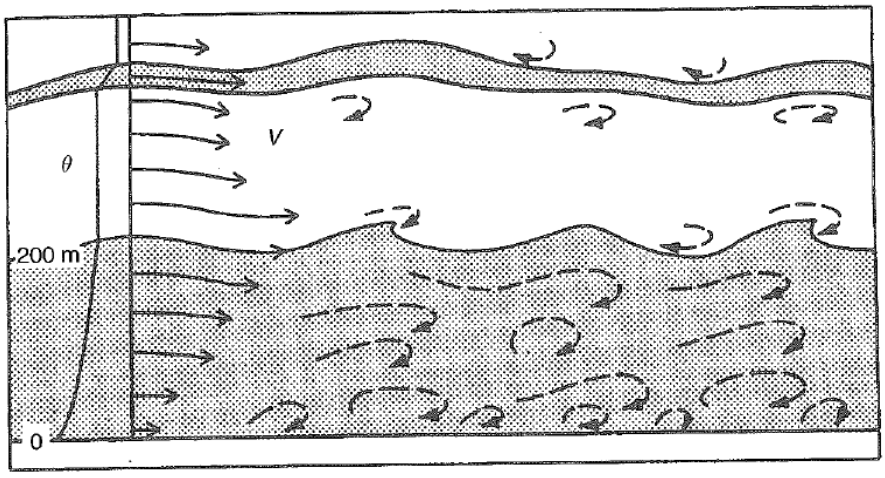

Figure 3. Artistic rendering of an idealized nocturnal PBL. Note its reduced depth (~200 m) relative to the daytime PBL in Figure 2 (~1500 m). In the nocturnal PBL, turbulence results exclusively from vertical wind shear. A pronounced low-level jet exists atop the nocturnal PBL and is theorized to result from inertial oscillations induced by an imbalance between the Coriolis and horizontal pressure gradient forces that develops as radiative cooling acts to decouple the surface layer from the atmosphere above. Gravity waves trapped beneath the near-surface inversion are superimposed upon the mean flow, and the weakly turbulent residual mixed layer is found above this inversion. Figure reproduced from Stensrud (2007), their Figure 5.7.

PBL Structure

The temporal evolution of the daytime PBL is depicted in Figure 4. Conceptual vertical profiles of potential temperature, momentum, and moisture within the daytime PBL are presented in Figure 5, while their nighttime PBL counterparts are depicted in Figure 6.

Vertical mixing in the PBL *homogenizes* potential temperature, mixing ratio, and momentum. As potential temperature is increased both by sensible heat fluxes from beneath during the day and by entrainment of warmer air from above the PBL, vertical profiles of potential temperature within the PBL are typically uniform. Latent heat fluxes from beneath during the day typically act to increase mixing ratio whereas entrainment of air from above the PBL typically acts to decrease mixing ratio. As a result, mixing ratio typically decreases slightly with increasing height within the PBL. Momentum, often viewed in the context of wind speed, is often well-mixed in the PBL, particularly when the synoptic-scale horizontal pressure gradient is weak and above the surface layer. When this is not true, however, momentum may not appear well-mixed.

At night, radiative cooling results in the surface layer decoupling from the mixed layer above. In the resulting stable layer, potential temperature, mixing ratio, and wind speed all typically increase

with height. Atop this stable layer is the residual mixed layer, where potential temperature, mixing ratio, and wind speed are approximate constant with height, as in the daytime PBL. As noted in the Figure 2 caption, the residual layer slowly and episodically shrinks in depth through the night as the near-surface stable layer deepens (due to continued radiative cooling) and internal friction erodes it from the top-down. Profiles of potential temperature, mixing ratio, and wind speed above the nocturnal PBL, in the free atmosphere, closely resemble their daytime counterparts.

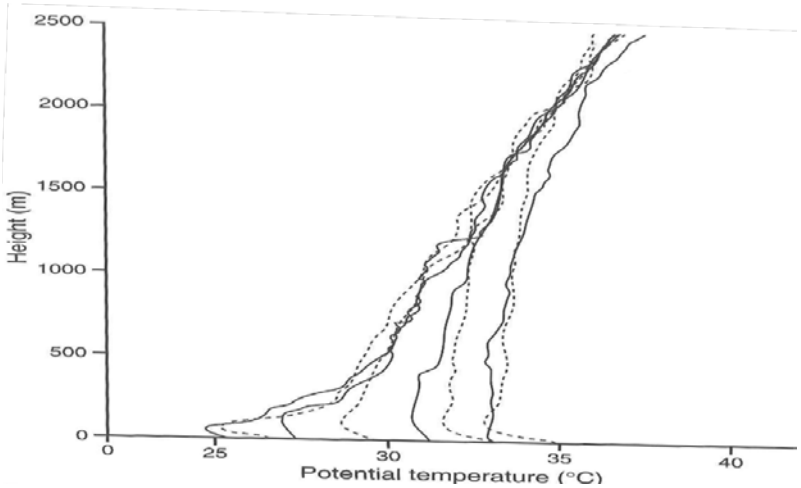

Figure 4. Vertical profiles of potential temperature (°C). Solid lines depict profiles obtained over a salt flat, while dashed lines depict profiles obtained over a vegetated yet sandy location. Profiles taken early (late) on this day are located further to the left (right) on the diagram. Figure reproduced from Warner (2011), their Figure 4.10.

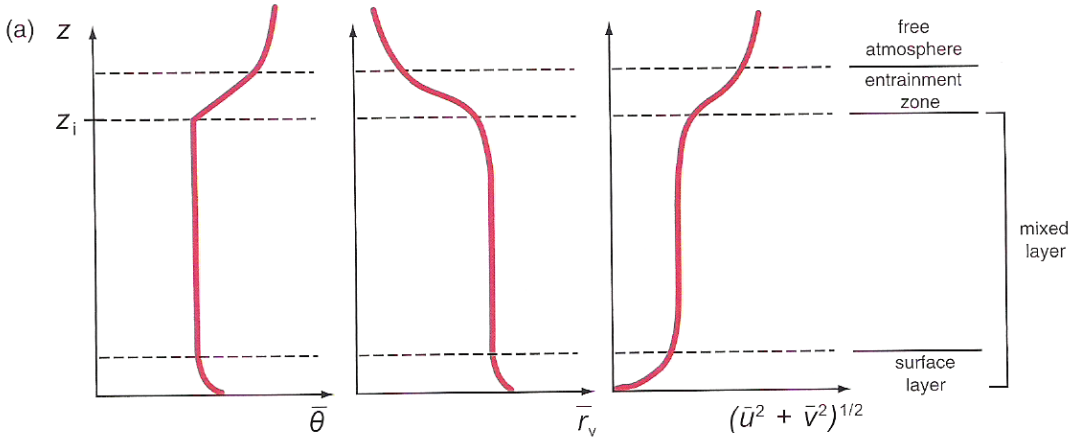

Figure 5. Conceptualized vertical profiles of potential temperature, water vapor mixing ratio, and horizontal wind speed over the depth of the daytime PBL. Figure reproduced from Markowski and Richardson (2010), their Figure 4.11a.

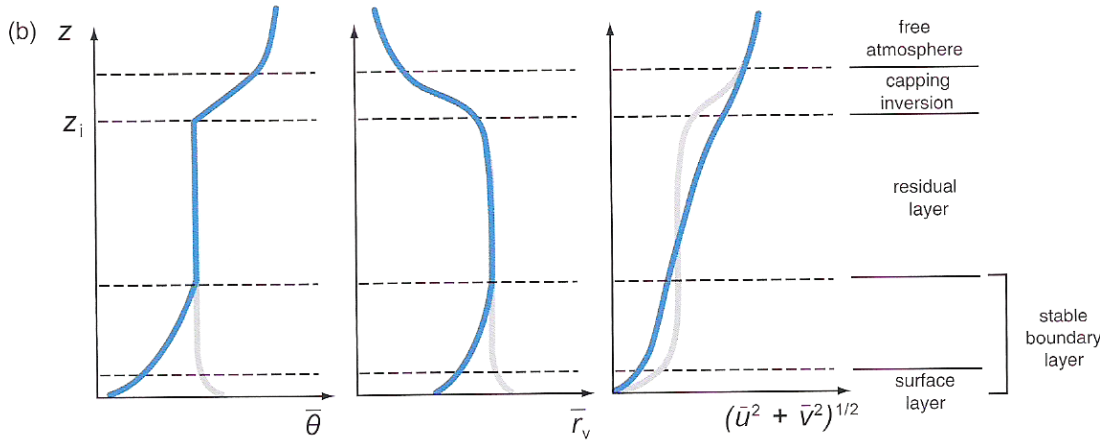

Figure 6. As in Figure 5, except for the nighttime PBL. Thin grey lines in each panel depict their daytime PBL counterparts for comparison. Figure reproduced from Markowski and Richardson (2010), their Figure 4.11b.

Within the PBL exists three distinct layers. The discussion to this point has focused on the *mixed layer*, which is the deepest of the three layers within the PBL and that which lies closes to the free atmosphere. Below the mixed layer is the *surface layer*. The surface layer, with thickness of ~100 m or less, is a layer over which turbulent transports vary little in magnitude with height relative to their variability within the mixed layer above. Within this layer, potential temperature decreases with height from its relative maximum at the surface that results from strong sensible heating. The resulting lapse rate is superadiabatic. Mixing ratio also decreases with height from its relative maximum at the surface that results from surface latent heat fluxes. Momentum, however, increases with height from its relative minimum at the surface that results from friction. Surface layer processes are typically parameterized by a surface layer parameterization, which is often developed and tuned to work with a particular PBL parameterization.

Below the surface layer, and nearest the surface, is the *laminar sublayer*. Because the wind speed perpendicular to any rigid surface such as the ground must be zero, turbulence cannot exist right at the ground. In the absence of turbulence, some other means of transporting sensible and latent heat fluxes from the underlying surface to the boundary layer above must exist. This occurs via molecular mixing within the laminar sublayer, which has a thickness of approximately 1 mm. Transport via molecular mixing is downgradient, from high to low values, and thus acts to reduce vertical gradients in potential temperature and mixing ratio that exist between the surface and the air just above. Physical processes occurring in the laminar sublayer are typically parameterized in one or both of surface layer and land-surface parameterizations.

As stated above, PBL structure is strongly impacted by the characteristics of the underlying surface. This is particularly manifest via the roughness of that surface, given by the *roughness length* (or z_0). The roughness length defines the height above the ground at which the mean wind

speed goes to zero under neutrally stable conditions. Roughness length is relatively small, on the order of millimeters, over relatively smooth surfaces and is relatively large, on the order of centimeters or larger, over relatively rough surfaces. The roughness length influences the vertical momentum profile within the surface layer, which in turn influences near-surface turbulent fluxes of heat, moisture, and momentum. For a well-mixed PBL, the vertical profile of momentum within the surface layer is a log-wind profile, as given by:

$$u(z) = \frac{u*}{k} \ln\left(\frac{z}{z_0}\right)$$

Here, $u*$ is the friction velocity, reflecting the drag (or frictional stress) of the surface against the atmosphere. Both $u*$ and k, the von Karman constant (typically 0.35-0.4), are independent of height. As a result, the horizontal wind speed – and thus momentum – increases logarithmically with increasing height above the ground within the surface layer. Though the log-wind profile explicitly holds only under neutrally stable conditions, similar profiles result from stable and unstable conditions.

Other PBL-Related Concepts

When we think of the PBL, we typically think of the local PBL. However, vertical profiles of potential temperature, mixing ratio, and momentum within the local free atmosphere may reflect properties of upstream PBLs that have been advected atop the local PBL by the synoptic-scale flow. These *elevated mixed layers* are most common downwind of large mountain ranges and, to lesser extent, over the tropical North Atlantic Ocean downwind of the Sahara Desert. Boundaries between the local PBL and an elevated mixed layer are known as *internal boundaries*. A PBL parameterization must be able to accurately represent the formation of both the local PBL and the elevated mixed layer, while the numerical model as a whole must be able to accurately depict the downstream transport and evolution of the elevated mixed layer. An idealized schematic of an elevated mixed layer, such as might occur over the Great Plains downwind of the Rocky Mountains, is depicted in Figure 7.

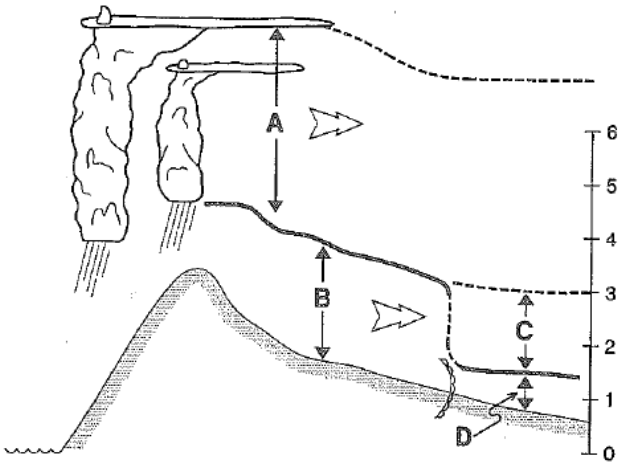

Figure 7. Idealized schematic of some of the complex structures that PBL parameterizations must be able to accurately represent. In this example, a shallow, moist PBL (D) is found ahead of a dryline. Behind the dryline, strong sensible heating results in a deep, well-mixed PBL with low relative humidity (B). The synoptic-scale west-to-east flow advects this layer over that in (D), resulting in the formation of an elevated mixed layer (C). A similar structure results when a mixed layer such as that in (B) is advected over a comparatively cool, moist marine layer. The downstream vertical profile can also be influenced by upstream processes over elevated terrain – here, deep, moist convection and concordant latent heat release (A). Figure reproduced from Stensrud (2007), their Figure 5.8.

Further, vertical mixing in the PBL exerts a control upon surface temperature and moisture. Indeed, a common rule of thumb for forecasting high temperatures during sunny days in the warm season is to follow a dry adiabat from the midday forecast 850 hPa temperature down to the surface. As a dry adiabat is a line of constant potential temperature, this rule follows from the principle that vertical mixing acts to homogenize potential temperature in the PBL. If a superadiabatic lapse rate immediately above the surface is anticipated, such as if the underlying soils are dry, then adding 1-2°C to the temperature obtained from this rule often leads to improved results. Vertical mixing also influences lifting and stability parameters such as the lifting condensation level, level of free convection, and CAPE and CIN. This exerts a control on both diurnal cumulus cloud development and thunderstorm formation. Finally, vertical mixing also influences surface winds, most notably when strong winds are found atop the PBL and strong surface sensible heating occurs.

Finally, although the PBL is governed by local turbulence, larger-scale phenomena regularly emerge from and interact with the local turbulence. The most commonly observed manifestation of larger-scale PBL variability is that associated with *roll circulations*. Rolls are most commonly observed during the daytime PBL during the warm season, when sensible heating is strong, but can also be observed in the nocturnal PBL as well as the daytime PBL during the cold season.

Rolls are typically organized parallel to the mean horizontal wind within the PBL and can be analyzed using visible satellite imagery or Doppler radar.

PBL Parameterization: Is It Even Necessary?

Though the above discussion might not indicate this to be the case, the primitive equations are capable of explicitly resolving turbulent motions within the atmosphere if effective radiation and land-surface parameterizations are present within the model (e.g., to represent local buoyancy, surface heat fluxes, and surface drag). However, as turbulent eddies cover a wide range of length scales ranging from tens of meters to a kilometer or more, to do so within a numerical model is computationally expensive. Approaches exist by which a PBL parameterization need not be used, such as large eddy and direct numerical simulation. The latter explicitly resolves all turbulent flows, whereas the former only does so for relatively large eddies. Large eddy simulation has been used to guide the development and evaluation of PBL parameterizations. The computational expense of these methods, however, currently limits the extent to which they are used in real-time and most research-focused simulations. As a result, a PBL parameterization is needed to represent the resolved-scale impacts of sub-grid-scale turbulence within a numerical simulation.

An Introduction to PBL Parameterization: Turbulence Closure

Early in the semester, we introduced the concept of *Reynolds' averaging* to rewrite the primitive equations so that they are formally valid only on the scales resolved by the model grid. A model dependent variable x can be written as the sum of a resolved-scale mean value $\bar{x}$ and a sub-grid-scale perturbation value x'. Substituting this definition into the primitive equations and using *Reynolds' postulates* to simplify the result allows one to obtain a form of the primitive equations applicable only on the scales resolved by the model grid.

Let us revisit Reynolds' averaging in the context of the v-momentum equation. Neglecting the curvature terms and friction for convenience, the v-momentum equation may be written as:

$$\frac{\partial v}{\partial t} = -u\frac{\partial v}{\partial x} - v\frac{\partial v}{\partial y} - w\frac{\partial v}{\partial z} - \frac{1}{\rho}\frac{\partial p}{\partial y} - 2\Omega u \sin\phi$$

If we rewrite u, v, w, p, and ρ as the sum of their resolved-scale and sub-grid-scale components, noting that $\rho' \approx 0$, then we obtain:

$$\frac{\partial \bar{v}}{\partial t} + \frac{\partial v'}{\partial t} = -\left(\bar{u}+u'\right)\frac{\partial\left(\bar{v}+v'\right)}{\partial x} - \left(\bar{v}+v'\right)\frac{\partial\left(\bar{v}+v'\right)}{\partial y} - \left(\bar{w}+w'\right)\frac{\partial\left(\bar{v}+v'\right)}{\partial z} - \frac{1}{\bar{\rho}}\frac{\partial\left(\bar{p}+p'\right)}{\partial y} - 2\Omega\left(\bar{u}+u'\right)\sin\phi$$

Expanding this equation, we obtain:

$$\frac{\partial \bar{v}}{\partial t}+\frac{\partial v'}{\partial t}=-\bar{u}\frac{\partial \bar{v}}{\partial x}-\bar{u}\frac{\partial v'}{\partial x}-u'\frac{\partial \bar{v}}{\partial x}-u'\frac{\partial v'}{\partial x}-\bar{v}\frac{\partial \bar{v}}{\partial y}-\bar{v}\frac{\partial v'}{\partial y}-v'\frac{\partial \bar{v}}{\partial y}-v'\frac{\partial v'}{\partial y}-\bar{w}\frac{\partial \bar{v}}{\partial z}-\bar{w}\frac{\partial v'}{\partial z}-w'\frac{\partial \bar{v}}{\partial z}-w'\frac{\partial v'}{\partial z}$$
$$-\frac{1}{\bar{\rho}}\frac{\partial \bar{p}}{\partial y}-\frac{1}{\bar{\rho}}\frac{\partial p'}{\partial y}-2\Omega\bar{u}\sin\phi-2\Omega u'\sin\phi$$

If we take the Reynolds average of this equation and apply Reynolds' postulates, we obtain:

$$\frac{\partial \bar{v}}{\partial t}=-\bar{u}\frac{\partial \bar{v}}{\partial x}-\bar{v}\frac{\partial \bar{v}}{\partial y}-\bar{w}\frac{\partial \bar{v}}{\partial z}-\overline{u'\frac{\partial v'}{\partial x}}-\overline{v'\frac{\partial v'}{\partial y}}-\overline{w'\frac{\partial v'}{\partial z}}-\frac{1}{\bar{\rho}}\frac{\partial \bar{p}}{\partial y}-2\Omega\bar{u}\sin\phi$$

The fourth, fifth, and sixth terms on the right-hand side of this equation, which represent the advection of *v'* by **v'** (e.g., advection of turbulent meridional velocity by turbulent velocity), may be rewritten using the flux-form definitions:

$$\frac{\partial \overline{u'v'}}{\partial x}=\overline{u'\frac{\partial v'}{\partial x}}+\overline{v'\frac{\partial u'}{\partial x}} \qquad \frac{\partial \overline{v'v'}}{\partial y}=\overline{v'\frac{\partial v'}{\partial y}}+\overline{v'\frac{\partial v'}{\partial y}} \qquad \frac{\partial \overline{w'v'}}{\partial z}=\overline{w'\frac{\partial v'}{\partial z}}+\overline{v'\frac{\partial w'}{\partial z}}$$

But, on turbulent scales of motion, wherein the Boussinesq approximation is said to hold, the following continuity equation applies:

$$\frac{\partial u'}{\partial x}+\frac{\partial v'}{\partial y}+\frac{\partial w'}{\partial z}=0$$

If this equation is multiplied by *–v'* and Reynolds averaged, we find that three of the six terms in the flux-form expansion above drop out. This allows us to rewrite our *v*-momentum equation:

$$\frac{\partial \bar{v}}{\partial t}=-\bar{u}\frac{\partial \bar{v}}{\partial x}-\bar{v}\frac{\partial \bar{v}}{\partial y}-\bar{w}\frac{\partial \bar{v}}{\partial z}-\frac{\partial \overline{u'v'}}{\partial x}-\frac{\partial \overline{v'v'}}{\partial y}-\frac{\partial \overline{w'v'}}{\partial z}-\frac{1}{\bar{\rho}}\frac{\partial \bar{p}}{\partial y}-2\Omega\bar{u}\sin\phi$$

Every term in this equation excepting the fourth, fifth, and sixth terms on the right-hand side is written in terms of only resolved-scale variables. These terms require no parameterization. The remaining terms, mathematically representing covariances and physically representing the grid-scale-averaged turbulent fluxes, must be parameterized in some fashion.

PBL parameterizations differ in how these terms are parameterized. Two approaches exist:

- Directly parameterize these terms in terms of some empirical relationships between these terms and resolved-scale model variables.
- Develop predictive equations for these terms.

The first of these methods is straightforward to conceptualize, and we will return to it shortly when considering examples of PBL parameterization. In contrast, the second of these methods is not as straightforward to conceptualize. How, exactly, can predictive equations be developed for the covariance terms in the above equation? To do so, we require two forms of the *v*-momentum equation: its final, simplified form and its fully-expanded form:

$$\frac{\partial \bar{v}}{\partial t} = -\bar{u}\frac{\partial \bar{v}}{\partial x} - \bar{v}\frac{\partial \bar{v}}{\partial y} - \bar{w}\frac{\partial \bar{v}}{\partial z} - \frac{\partial \overline{u'v'}}{\partial x} - \frac{\partial \overline{v'v'}}{\partial y} - \frac{\partial \overline{w'v'}}{\partial z} - \frac{1}{\bar{\rho}}\frac{\partial \bar{p}}{\partial y} - 2\Omega\bar{u}\sin\phi$$

$$\begin{aligned}\frac{\partial \bar{v}}{\partial t} + \frac{\partial v'}{\partial t} = &-\bar{u}\frac{\partial \bar{v}}{\partial x} - \bar{u}\frac{\partial v'}{\partial x} - u'\frac{\partial \bar{v}}{\partial x} - u'\frac{\partial v'}{\partial x} - \bar{v}\frac{\partial \bar{v}}{\partial y} - \bar{v}\frac{\partial v'}{\partial y} - v'\frac{\partial \bar{v}}{\partial y} - v'\frac{\partial v'}{\partial y} - \bar{w}\frac{\partial \bar{v}}{\partial z} - \bar{w}\frac{\partial v'}{\partial z} - w'\frac{\partial \bar{v}}{\partial z} - w'\frac{\partial v'}{\partial z} \\ &- \frac{1}{\bar{\rho}}\frac{\partial \bar{p}}{\partial y} - \frac{1}{\bar{\rho}}\frac{\partial p'}{\partial y} - 2\Omega\bar{u}\sin\phi - 2\Omega u'\sin\phi\end{aligned}$$

If we subtract the top equation from the bottom equation, we obtain:

$$\begin{aligned}\frac{\partial v'}{\partial t} = &-\bar{u}\frac{\partial v'}{\partial x} - u'\frac{\partial \bar{v}}{\partial x} - u'\frac{\partial v'}{\partial x} - \bar{v}\frac{\partial v'}{\partial y} - v'\frac{\partial \bar{v}}{\partial y} - v'\frac{\partial v'}{\partial y} - \bar{w}\frac{\partial v'}{\partial z} - w'\frac{\partial \bar{v}}{\partial z} - w'\frac{\partial v'}{\partial z} - \frac{1}{\bar{\rho}}\frac{\partial p'}{\partial y} - 2\Omega u'\sin\phi \\ &+ \frac{\partial \overline{u'v'}}{\partial x} + \frac{\partial \overline{v'v'}}{\partial y} + \frac{\partial \overline{w'v'}}{\partial z}\end{aligned}$$

This equation can be used in part to obtain equations for the covariance terms. For instance, the general form of a predictive equation for $\overline{u'v'}$ is given by its chain rule expansion:

$$\frac{\partial}{\partial t}\left(\overline{u'v'}\right) = \overline{u'\frac{\partial v'}{\partial t}} + \overline{v'\frac{\partial u'}{\partial t}}$$

The first right-hand side term of this equation can be obtained from the tendency equation for *v'* by multiplying it by *u'*, applying the product rule for partial derivatives, taking a Reynolds average, and simplifying using the continuity equation and Reynolds' postulates. The second right-hand side term can be obtained similarly from the tendency equation for *u'* from an analogous expansion of the *u*-momentum equation.

However, when doing so, triple correlation terms of the form $\overline{u'u'v'}$, $\overline{u'v'v'}$, and $\overline{u'w'v'}$ result. One could follow a similar procedure to obtain predictive equations for the triple correlation terms, but these would contain quadruple correlation terms. Indeed, one can never obtain a predictive equation for a correlation term that does not contain an even higher-order correlation term. At some point, the unknown higher-order correlation terms must be parameterized in terms of the resolved-scale model variables.

The *order* of a PBL parameterization is defined by the lowest order of covariance or correlation terms that are parameterized. A first-order closure means that there exist predictive equations for the resolved-scale model variables while the covariance terms are parameterized. A second-order closure means that there exist predictive equations for the resolved-scale model variables and the covariance terms while the triple correlation terms are parameterized. Higher-order closures follow this same basic pattern. Non-integer closures, wherein a mixture of parameterizations and predictive equations are used to solve for sub-grid-scale covariance terms, also exist. Generally, higher-order closures are thought to be more accurate because they reduce the influence that the parameterized terms have upon the resolved-scale model fields. For those parameterizations in which vertical mixing is parameterized as being proportional to diffusion coefficients, higher-order closures also allow for the more accurate specification of the diffusion coefficients.

Within this hierarchy of PBL parameterization orders is the approach used to parameterize the sub-grid-scale turbulence. Two approaches exist: *local* and *non-local closures*. Local closures use only known (resolved) quantities at adjacent vertical grid points to obtain values of unknown quantities. By contrast, non-local closures use known quantities over the depth of the PBL to obtain values of unknown quantities. Local closures are formulated under the assumption that turbulent mixing occurs primarily by turbulent eddies of small vertical extent, whereas non-local closures assume that turbulent mixing occurs by eddies of varying vertical extent. Two common non-local closures assume (a) turbulent mixing occurs by turbulent eddies of varying depth with roots in the surface layer or (b) turbulent mixing occurs by turbulent eddies of varying depth with roots anywhere within the PBL. Idealized schematics of local and non-local closures are depicted in Figure 8. The Mellor-Yamada-Janjic and Yonsei University PBL parameterizations are examples of local and non-local closures, respectively. Note that a PBL parameterization need not be exclusively local or non-local; for instance, the ACM2 PBL parameterization is non-local for upward mixing and local for downward mixing.

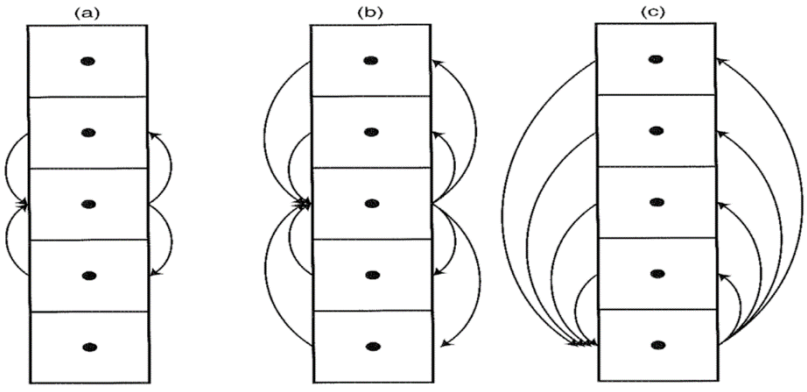

Figure 8. Idealized schematics of vertical mixing associated with (a) local, (b) non-local rooted at any grid cell, and (c) non-local rooted in the surface layer closures. Please see above for more details regarding each closure. Figure reproduced from Warner (2011), their Figure 4.15.

Local Turbulence Closure

As noted above, local turbulence closures use only known quantities at adjacent vertical grid points to obtain values of unknown quantities. They are formulated under the assumption that turbulent mixing occurs primarily by turbulent eddies of small vertical extent. To begin, let us assume a first-order local turbulence closure, such that the covariance terms are those that are parameterized, and focus on vertical mixing within the daytime PBL when buoyancy is important.

The covariance terms, defining vertical fluxes, take the general parameterized form of:

$$\overline{w'\xi'} = -K\frac{\partial\overline{\xi}}{\partial z}$$

Here, ξ is any model dependent variable (e.g., u, v, θ, q) for which a covariance term exists and K is a diffusion (or mixing) coefficient with units of $m^2\ s^{-1}$. Typically, different values for K are specified for momentum (K_m) and mass (K_h) turbulent mixing. Similar equations can be obtained for higher-order closure parameterizations; e.g., the left-hand side may be associated with a triple correlation term that is parameterized as a function of the product of a diffusion coefficient with a vertical partial derivative of a resolved double correlation (or covariance) term.

The above equation contains two important insights:

- The covariance term is parameterized as a function of predicted model variables.
- As the partial derivative is defined by the limit as Δz approaches zero (i.e., infinitesimally small Δz), this formulation is inherently local.

To gain insight into this parameterization, let us consider the vertical heat flux, i.e.,

$$\overline{w'\theta'} = -K_h\frac{\partial\overline{\theta}}{\partial z}$$

Let us also consider an idealized vertical profile of $\overline{\theta}$ within the daytime PBL, as in Figure 5a. In the daytime surface layer, where $\overline{\theta}$ decreases with height due to strong sensible heating of the underlying surface, the parameterization indicates that $\overline{w'\theta'} > 0$ for $K_h > 0$. This implies a positive correlation between w', representing vertical motions associated with turbulent eddies, and θ'. Turbulence thus acts to move warm air ($\theta' > 0$) upward ($w' > 0$) or cool air downward. This is consistent with what we know about the daytime surface layer: thermals act to transport warmth upward, from relatively high values toward relatively low values.

At the top of the daytime PBL, where there exists an inversion and thus a rapid increase in $\overline{\theta}$ with height, the parameterization indicates that $\overline{w'\theta'} < 0$ for $K_h > 0$. This implies a negative correlation

between w' and θ'. Turbulence thus acts to move warm air ($\theta' > 0$) downward ($w' < 0$) or cool air upward. This is consistent with what we know about the daytime mixed layer: turbulent eddies entrain high potential temperature air from above into the boundary layer, again representing transport from relatively high values toward relatively low values.

The above discussion helps to illustrate that, so long as $K > 0$, this parameterized turbulence is associated with *downgradient* transport – i.e., that from high values toward low values. However, not all turbulent transport within the PBL is downgradient. Consider the case of the late morning PBL, characterized by a residual nocturnal inversion atop a shallow superadiabatic layer associated with sensible heating of the underlying surface. In the real atmosphere, warm thermals move heat upward from the surface over the depth of the PBL (e.g., Figure 2), including through the residual nocturnal inversion. In the context of a local gradient, this can be thought of as *countergradient* transport, or that from low toward high values. However, the first-order local closure instead actually represents this as downgradient downward transport of warm air.

Thus, there exists an inconsistency between this parameterization and the underlying physics. This is a problem, as observations of the daytime PBL indicate that most vertical transport of mass and momentum is accomplished by the largest eddies *that are more representative of the properties of the entire PBL rather than the local properties* (i.e., those at adjacent vertical levels). This implicitly indicates that not all vertical transport within the daytime PBL is downgradient. Higher-order local closure parameterizations do permit countergradient transport but do not permit large eddies and thus are a crude approximation to the underlying physics.

Returning to Figure 5a, let us consider the daytime mixed layer. Here, where $\overline{\theta}$ is approximately constant with height, the parameterization indicates that $\overline{w'\theta'} \approx 0$ for $K_h > 0$. This implies no vertical heat flux – and thus no turbulence – in the daytime mixed layer. However, observations indicate that the daytime mixed layer is characterized by strong thermals and associated turbulent eddies that span the depth of the PBL (e.g., Figure 2). Thus, the inability of local closure parameterizations to *explicitly* resolve transport by large eddies limits their realism.

Local closure parameterizations require some means of specifying the mass and momentum diffusion coefficients applicable to the terms that are parameterized. The precise methods by which these coefficients are specified varies between local closures, whether first-order or higher-order in nature. For first-order local closures, K_h and K_m are typically functions of an empirically-determined mixing length scale, vertical wind shear, and stability; in other words, the phenomena believed to result in, or be a result of, turbulence within the daytime or nocturnal PBL. For higher-order local closures, the diffusion coefficients can also be functions of predicted covariance terms, such as those that describe turbulent kinetic energy and potential temperature variance. Overall, expressions for the diffusion coefficients are generally derived empirically from comparison to observations or large-eddy simulations.

Non-Local Turbulence Closure

Non-local closures use known quantities over the depth of the PBL to obtain values of unknown quantities and, thus, are more consistent with observations as they do not assume that turbulent mixing occurs primarily by turbulent eddies of small vertical extent. Non-local turbulent mixing can take multiple forms, two of which are depicted in Figure 8. As one might expect, non-local parameterizations differ with respect to how large eddies and their effects are parameterized.

One conceptually straightforward method of non-local closure parameterization is that which is used within the NCEP Global Forecast System (GFS) model. A variation of this parameterization is given by the Yonsei University (YSU) parameterization available in the WRF-ARW model. Here, the covariance terms for vertical fluxes take the general form:

$$\overline{w'\xi'} = -K\left(\frac{\partial\overline{\xi}}{\partial z} - \gamma_{\xi}\right)$$

γ_{ξ} is a correction, applied to the local gradient formulation, that accounts for turbulent mixing by large eddies. In the GFS model, this correction applies only to the mass variables (heat, moisture) within the PBL; otherwise, the correction term is set to zero. Where this correction term is zero, the formulation is identical to a local closure. As a result, this non-local parameterization may be thought of as a 'corrected' local closure parameterization.

The empirical correction term takes the form:

$$\gamma_{\xi} = 7.8\frac{\overline{(w'\xi')_{sfc}}}{w_s}$$

Here, w_s is the mixed layer velocity scale, which is a function of the surface friction velocity u_{sfc}* and the wind profile evaluated at the top of the surface layer. The value for $\overline{(w'\xi')_{sfc}}$, here defining a surface heat or moisture flux (as this parameterization does not apply the correction to momentum), is obtained from the surface layer parameterization. Consequently, this non-local parameterization is one in which large eddies are assumed to be rooted in the surface layer, analogous to Figure 8c.

K – specifically that for momentum, but also indirectly for mass variables – is a function of the height above the ground z, the mixed layer velocity scale w_s, and the height of the PBL h. The height of the PBL is determined iteratively and is a function of the horizontal wind speed at the top of the PBL, the virtual potential temperature at the first model level, and the difference in virtual potential temperature between the top of the PBL and the surface.

Non-local closures that do not take the form of 'corrected' local closure parameterizations may also be formulated. The Blackadar scheme is an example of one such closure in which vertical mixing is assumed to be rooted within the surface layer, as in Figure 8c. Here, the intensity of turbulent vertical mixing is a function of the surface layer potential temperature (θ_{sl}) and heat flux at the top of the surface layer. This leads to the following expression for the θ time tendency in the PBL:

$$\frac{\partial\theta(z)}{\partial t} = \overline{m}\left[\theta_{sl} - \theta(z)\right]$$

Instead of being a function of the change in some model variable between adjacent model levels, here the parameterization is a function of the change in some model variable between the surface layer and the model level in question, and it operates directly on the potential temperature tendency (rather than a correlation term that, in turn, appears in the potential temperature tendency equation). Despite similar mathematics, the physical underpinnings are quite different between this and the previously-considered closure parameterizations.

In the above, $\overline{m}$ is the fraction of mass exchanged between the boundary layer and the free atmosphere above. It is a function of the heat flux at the top of the surface layer, an entrainment coefficient, and the integrated difference (from the top of the surface layer to the top of the PBL) between the surface layer and model layer potential temperatures. The surface layer potential temperature is a function of the difference in heat fluxes into (from below) and out of (to above) the surface layer.

A related formulation drops the assumption that all vertical mixing is rooted within the surface layer. It is formulated similarly to the above, albeit with increased dimensionality from the need to represent mixing between vertical layers of different depths at different altitudes. An idealized schematic of non-local vertical mixing within this formulation is depicted in Figure 8b.

Interactions Between PBL and Other Parameterizations

A PBL parameterization must interact with several other physical parameterizations. Surface roughness is conveyed through land-use data provided to a land-surface parameterization. Latent and sensible heat fluxes are modulated both by properties of the underlying surface, as reflected by soil type, soil temperature, and soil moisture, and by shortwave radiation, as manifest through both the diurnal cycle as well as cloud effects. Accurate representation of the interface between the mixed layer and the surface layer beneath it requires that PBL parameterizations effectively interact with surface layer parameterizations. Furthermore, although the two do not interact with each other, it is helpful to keep in mind that horizontal diffusion is used to represent horizontal

mixing above the PBL whereas a PBL parameterization is used to represent all mixing within the PBL and only vertical mixing above the PBL.

Practical Examples of Forecast Sensitivity to PBL Parameterization

There exist numerous published works in which forecast sensitivity to the choice of PBL parameterization has been evaluated. Here, we focus on a small subset of these works.

(1) General aspects of local and non-local closures

Evaluations of simulated PBLs from local and non-local closure parameterizations indicate that vertical mixing, relative to observations, tends to be underrepresented by local closures and overrepresented by non-local closures. This implies that local closures are associated with too little entrainment from the free atmosphere while non-local closures are associated with too much entrainment from the free atmosphere. For local closures, this results in relatively shallow PBLs that are too cool and moist, and thus too energetic (e.g., surface-based CAPE and CIN), relative to observations. For non-local closures, this results in relatively deep PBLs that are too warm and dry, and thus less energetic, relative to observations.

Illustrative examples of this behavior are given by Bright and Mullen (2002, *Wea. Forecasting*) for daytime warm-season PBLs over Arizona (Figure 9) and Stensrud and Weiss (2002, *Wea. Forecasting*) for the daytime PBL in advance of the 3 May 1999 Oklahoma tornado outbreak (Figure 10). Note that not all discrepancies from reality depicted in the simulated vertical profiles are exclusively associated with the chosen PBL parameterizations; inaccuracies in the initial conditions and other model system components also contribute.

Many subsequent investigators have obtained similar results to those depicted in Figures 9 and 10. The inability of local closures to explicitly resolve the large eddies responsible for the bulk of the mixing within the PBL is believed to be responsible for their behavior relative to both non-local closures and observations.

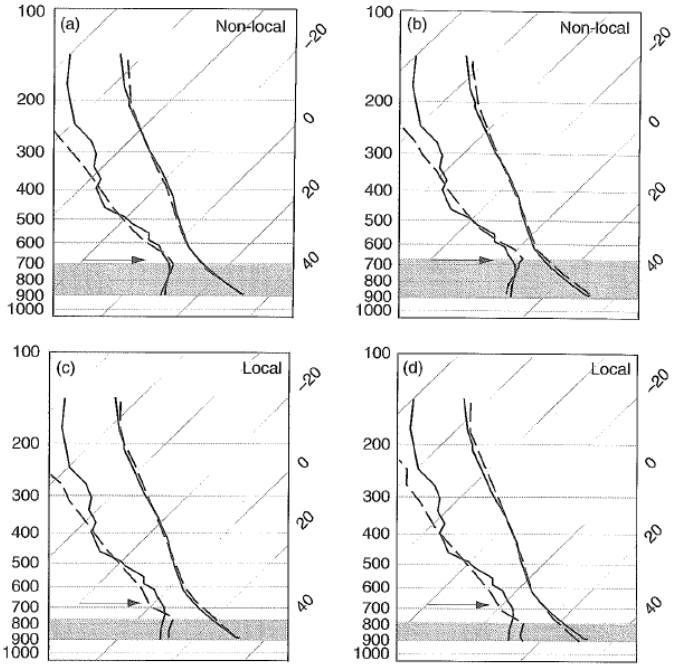

Figure 9. Simulated 12-h forecast composite soundings (dashed lines) valid at 0000 UTC at Tucson, AZ from (a,b) non-local and (c,d) local closure parameterizations. The verifying observed soundings are depicted by the solid black lines. Gray shading indicates simulated PBL depth, while the arrow denotes observed PBL depth. Figure reproduced from Stensrud (2007), their Figure 5.22, which was adapted from Figure 11 of Bright and Mullen (2002).

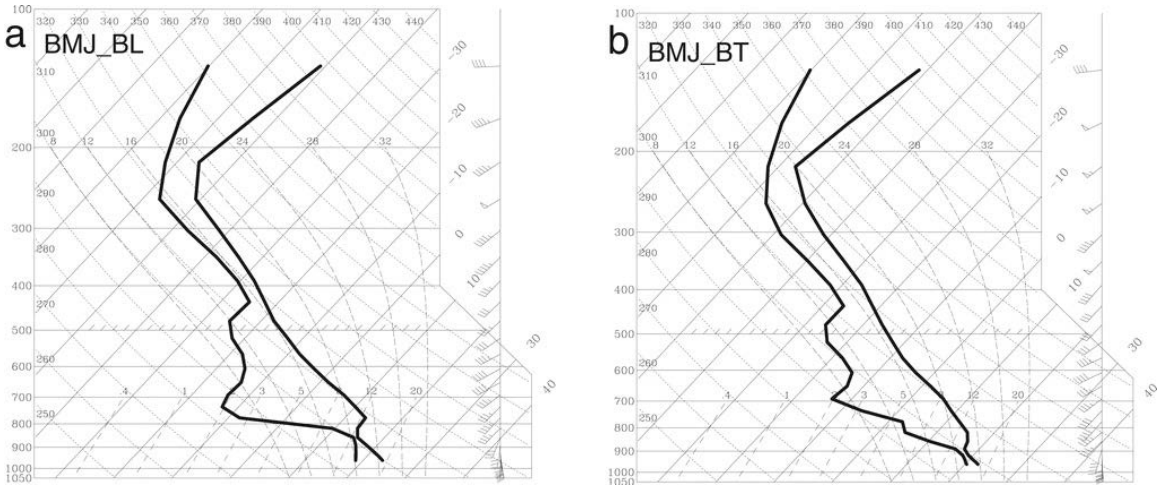

Figure 10. Simulated 24-h forecast soundings valid at 0000 UTC 4 May 1999 at Oklahoma City, OK from simulations utilizing a (a) non-local and (b) local closure parameterization. Figure reproduced from Stensrud and Weiss (2002), their Figure 8. The verifying sounding is available from the University of Wyoming Atmospheric Sounding archive.

(2) Dryline position: Clark et al. (2015, *Wea. Forecasting*)

Focusing upon warm-season environments known to support severe convection, Clark et al. (2015) examine sensitivity in dryline position to PBL parameterization. In the composite mean, all PBL parameterizations are associated with an eastward bias in dryline position relative to observations. Given the general insight in (1), it is perhaps not surprising that the magnitude of this bias is largest with non-local closures and smallest with local closures (Figure 11) as dryline position is a function of vertical mixing within the daytime PBL. An exception arises with the local closure Mellor-Yamada-Nakanishi-Niino parameterization, wherein strong vertical mixing contributed to a large eastward bias in the composite mean simulated dryline position. Errors in simulated composite vertical profiles of temperature, mixing ratio, and boundary layer depth generally follow from those described in (1) above.

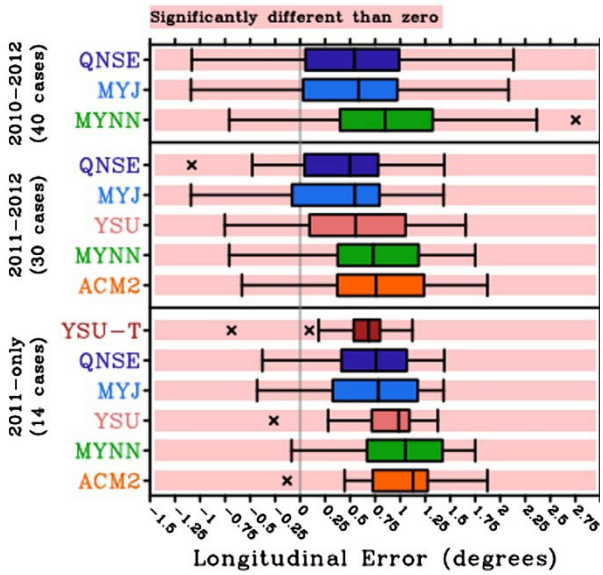

Figure 11. Box-and-whiskers plots of longitudinal error in simulated dryline position relative to observations (positive values denote an eastward bias) for simulations of warm-season environments supportive of thunderstorms. The median error is denoted by the solid vertical line through each box, which itself depicts the interquartile range. Outliers are defined as cases where the longitudinal error magnitude exceeds 1.5 times the interquartile range. The YSU and ACM2 schemes are non-local closures, whereas the MYJ, MYNN, and QNSE schemes are local closures. Figure reproduced from Clark et al. (2015), their Figure 6.

(3) Idealized tropical cyclone simulations: Hill and Lackmann (2009, *Mon. Wea. Rev.*)

Hill and Lackmann (2009, *Mon. Wea. Rev.*) examine sensitivity in the simulated maximum intensity of an idealized tropical cyclone to coupled planetary boundary layer and surface layer parameterizations. They find that the moisture exchange coefficient between the ocean and the atmosphere is larger with the surface layer model tied to the Mellor-Yamada-Janjic (MYJ) local

parameterization than with the surface layer model tied to the YSU non-local parameterization (Figure 12). This results in larger surface latent heat fluxes in the MYJ-based simulations. As surface latent heat fluxes are the primary energy source for tropical cyclones, this leads to stronger simulated tropical cyclones in the MYJ-based simulations relative to the YSU-based simulations.

Note that PBL parameterizations are typically designed, or tuned, to work with a specific surface layer model. How the surface layer model represents heat, moisture, and momentum exchange between the surface layer and the underlying surface exerts a significant control upon potential temperature, mixing ratio, and momentum within the surface layer. This impacts vertical mixing in both non-local and local closure parameterizations. Thus, PBL parameterization performance must be evaluated in light of both it and its accompanying surface layer parameterization.

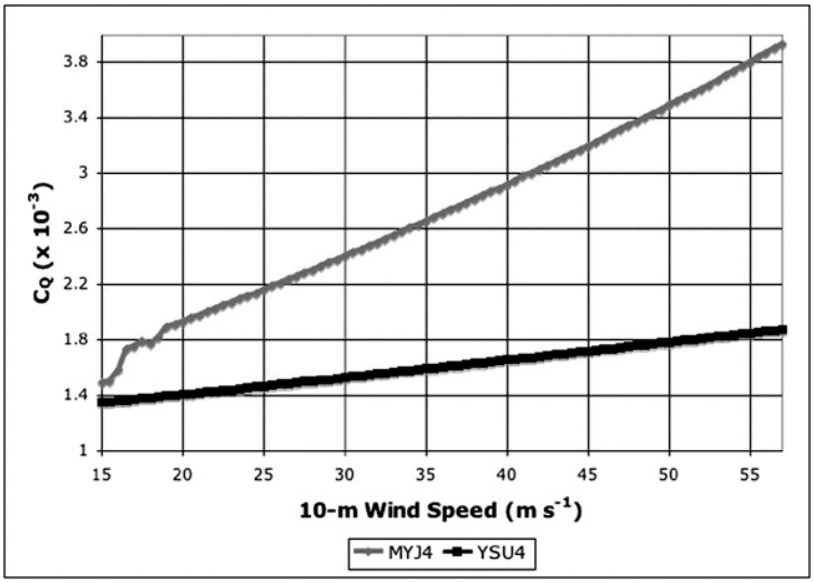

Figure 12. Moisture exchange coefficient (x10^{-3}; non-dimensional) as a function of 10-m wind speed (m s^{-1}) for the MYJ- (grey) and YSU-based (black) simulations. Figure reproduced from Hill and Lackmann (2009), their Figure 6.